Astronomy & Astrophysics

Anti-solar differential rotation on the active K-giant σ Geminorum
(Research Note)

Zs. Kővári[1], J. Bartus[2], K. G. Strassmeier[2], K. Vida[1,3], M. Švanda[4,5], and K. Oláh[1]

[1] Konkoly Observatory, 1525 Budapest, PO Box 67, Hungary
    e-mail: kovari@konkoly.hu
[2] Astrophysical Institute Potsdam, An der Sternwarte 16, 14482 Potsdam, Germany
    e-mail: [jbartus;kstrassmeier]@aip.de
[3] Eötvös University, Department of Astronomy, 1518 Budapest, PO Box 32, Hungary
    e-mail: vidakris@elte.hu
[4] Astronomical Institute, Faculty of Mathematics and Physics, Charles University in Prague, V Holešovičkách 2,
    18000 Prague 8, Czech Republic
    e-mail: svanda@asu.cas.cz
[5] Astronomical Institute, Academy of Sciences of the Czech Republic, v. v. i., Fričova 298, 25165 Ondřejov, Czech Republic

ABSTRACT

The active K1 giant σ Gem and its differential surface rotation is revisited. We refine our previous inconclusive result by recovering the spot migration pattern of this long-period RS CVn-type binary through application of the technique of "average cross-correlation of contiguous Doppler images" to a set of six Doppler images from 3.6 consecutive rotation cycles. We find an anti-solar differential rotation law with a shear of $\alpha \approx -0.022 \pm 0.006$. We also find evidence of a poleward migration trend of spots with an average velocity of ≈ 300 m s^{-1}.

Key words. stars: activity – stars: imaging – stars: late-type – stars: starspots – stars: individual: σ Geminorum

1. Introduction

The Sun is the only star for which surface differential rotation (DR) can be measured directly. A century ago, the first measurements of the solar DR were based on tracing the positions of sunspots at different latitudes (e.g. Maunder & Maunder 1905). The solar DR law and other plasma flows (such as meridional circulation or moat flow around sunspots) can be measured with astounding accuracy (e.g Shibahashi 2007; Švanda et al. 2007), largely due to space-borne solar and other long-term full-disk observations. Nevertheless, the underlying solar magnetic dynamo is still poorly understood, and thus the surface DR measurements for different type of stars could also provide useful input for our understanding of solar and stellar dynamos.

The detection of stellar surface differential rotation is still a difficult and challenging observational task. Starspots are regarded as an established assignation of solar-like active regions (magnetic concentrations) and are thus likely to be also suitable for tracking and recovering differential surface rotation and other surface flows. However, this tracer method is mainly conditioned by its initial surface reconstruction technique of Doppler imaging (e.g. Strassmeier et al. 2007). The method of cross-correlating consecutive Doppler images to follow the time evolution of the spots and to derive surface DR was demonstrated for the first time for the active star AB Dor (Donati & Collier Cameron 1997). Kővári et al. (2004) showed that consecutive Doppler images should be close enough in time to be cross-correlated because rapid spot motion and morphology evolution expeditiously covers up the traces of differential rotation.

In this paper we return to one of our former targets which was analysed in a series of Doppler-imaging papers, the rapidly-rotating K1-giant σ Gem, for which a time-series of six Doppler images was published by Kővári et al. (2001). We perform a more detailed analysis of these maps using our technique "average cross-correlation of contiguous Doppler images" (hereafter ACCORD) developed to filter out the masking effect of short-term spot changes. In Sect. 2 a summary of the Doppler images of σ Gem is given, then in Sect. 3 the technique ACCORD is described briefly. Our new findings on the DR and on a possibly poleward meridional flow are presented in Sect. 4, and results are discussed in Sect. 5.

2. Time-series Doppler images of σ Gem from 70 consecutive nights in 1996/97

σ Geminorum (75 Gem, HR 2973, HD 62044) is a long-period ($P_{\rm rot} \approx 20$ days) RS CVn-type system with a K1III primary star and an unseen companion star. A summary of its astrophysical parameters is given in Table 1. In our initial paper by Kővári et al. (2001), a time-series Doppler-imaging analysis was presented using 52 high-resolution optical spectra taken during a 70-night observing run at NSO/McMath in 1996/97. Spectra recorded two mapping lines, Ca I at 6439 Å and Fe I at 6430 Å. From these 52 spectra, a time-series of six data subsets was formed, each covering approximately one rotation period with half a rotation time-span between the successive subsets, i.e. half a rotation overlap. This way the whole observing time is 3.6 consecutive stellar rotations. For all subsets individual Doppler images were recovered from both mapping lines. Images #1, #3,

Table 1. Astrophysical data for σ Gem (adopted from Kővári et al. 2001).

Parameter	Value
Classification	K1 III
Distance (Hipparcos)	37.5 ± 1.1 pc
Luminosity, L	$52.5^{+14.5}_{-8.2}$ $L_\odot$
$\log g$	$2.5^{+0.23}_{-0.42}$
T_{eff}	4630 ± 100 K
$v \sin i$	27.5 ± 1 km s^{-1}
Inclination, i	$60° \pm 15°$
Period, $P_{\mathrm{rot}} = P_{\mathrm{orb}}$	19.60447 ± 0.00007 days
Orbital eccentricity, e	0.0
Radius, R	$12.3^{+1.6}_{-1.0}$ $R_\odot$
Chemical abundances	solar (adopted)

and #5, as well as #2, #4, and #6, all shown in our initial paper, represent contiguous stellar rotations and therefore uncorrelated maps. The Fe line provided a more detailed temperature reconstruction than the Ca line due to its narrower local line profile, although good agreement was achieved between the respective maps. Spotted regions were found either on the equator or at mid-latitudes but there were no spots at latitudes higher than $\approx 60°$. The time evolution of the maps were investigated by cross-correlating longitudinally the consecutive but contiguous image pairs, i.e., #1−#3, #2−#4, #3−#5 and #4−#6, but the correlation maps showed different patterns and this ambiguity was attributed to the masking effect of short-term spot changes.

3. Average cross-correlation of contiguous Doppler images

Straightforward comparisons of ccf maps can lead to inconclusive results (Weber 2004; Petit et al. 2004a). However, it is expected that averaging many ccf maps will emphasize common features, such as the surface DR pattern, and will diminish differences originating from individual spot evolution. On the other hand, simple averaging can also bleach the DR pattern, especially when the time baselines of the ccf maps (i.e. the time gap between the two Doppler images from which the ccf map is produced) are dissimilar. This is because the longitudinal shifts of the surface features in a ccf map are a linear function of the time span covered. To avoid such blurring, a linear normalisation (stretching or compressing parallel to the equator) must be done before the averaging. This step was missing from the previous study, which could have led to the inconclusive result. In this average ccf map, we then fit the correlation peak for each latitudinal stripe with a Gaussian profile. These Gaussian peaks per latitude then represent the DR pattern and can thus be fitted with a standard (solar-analogy driven) quadratic DR law:

$$\Omega(\beta) = \Omega_{\mathrm{eq}}\left(1 - \alpha \sin^2 \beta\right), \qquad (1)$$

where β is the stellar latitude, Ω_{eq} the equatorial angular velocity, and the surface shear parameter is defined as $\alpha = (\Omega_{\mathrm{eq}} - \Omega_{\mathrm{pole}})/\Omega_{\mathrm{eq}}$ where Ω_{pole} is the angular velocity near the pole. The latter is somewhat loosely defined as the very high latitude or nearly polar angular velocity.

This method was described and applied first to LQ Hya in Kővári et al. (2004), and then to IL Hya (Kővári et al. 2005) and to ζ And (Kővári et al. 2007). The most recent application of ACCORD is presented for UZ Lib by Vida et al. (2007).
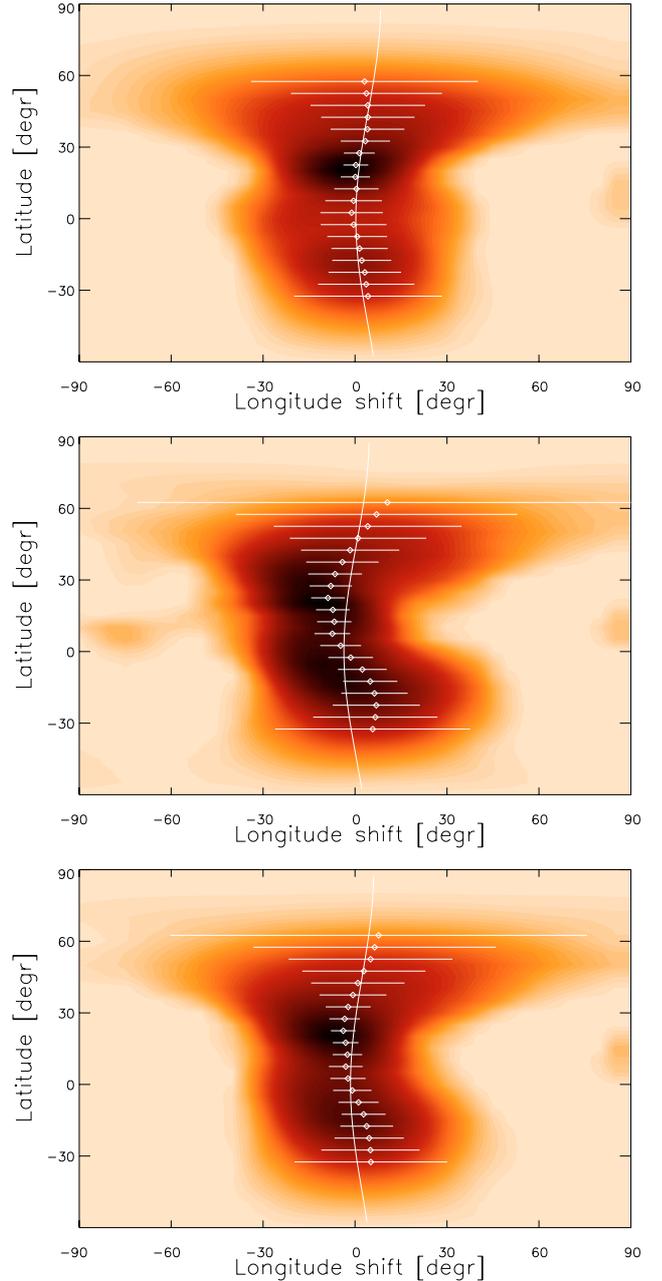
Fig. 1. Cross-correlation maps of σ Gem from ACCORD using the Ca images (*top panel*), the Fe images (*middle panel*), and their averages (*bottom panel*). The background grey scale is the strength of the correlation (white is no correlation, black is perfect correlation). The dots are the correlation peaks per 5°-latitude bin. Their error bars are defined as the FWHM of the Gaussian fit. Each ccf map recovers anti-solar differential rotation. See Table 2 for details.

4. Results

4.1. Anti-solar differential rotation

We apply ACCORD to our series of six Doppler images of σ Gem. Only the consecutive but contiguous image pairs are cross-correlated, i.e., #1−#3, #2−#4, #3−#5 and #4−#6. Maps from the Ca I-6439 line and the Fe I-6430 line, as well as their average (Ca+Fe) are used independently. The resulting ccf maps are shown in Fig. 1. The best-fit quadratic DR laws for the Gaussian peaks (dots) are overplotted as continuous lines with their error bars estimated from the FWHMs of the fitted

Table 2. Comparison of the DR laws obtained for σ Gem using different mapping lines. [†] The solar DR given for comparison was derived from tracing long-lived spots by Balthasar et al. (1986).

Maps used	Ω_{eq} [°/day]	$\Omega_{eq} - \Omega_{pole}$ [°/day]	α [–]	Lap time [days]
Ca I-6439	18.38 ± 0.02	-0.40 ± 0.07	-0.022 ± 0.004	≈ 900
Fe I-6430	18.18 ± 0.09	-0.41 ± 0.18	-0.022 ± 0.010	≈ 880
average (Ca+Fe)	18.29 ± 0.05	-0.38 ± 0.08	-0.021 ± 0.005	≈ 950
Sun[†]	13.46	2.98	0.22	120

Gaussians to the ccfs. Results agree well and suggest equatorial deceleration with an average surface shear of $\alpha \approx -0.022 \pm 0.006$. The error is the rms from the three mapping cases quoted in Table 2. The individual detections varied between $2.2-5.5\sigma$. $\Omega_{eq} - \Omega_{pole}$ translates into an average lap time of ≈ 900 days, i.e, the time the pole needs to overlap the equator by one full rotation. This is 7.5 times the solar value of 120 days, which results in one tenth of the solar surface shear (with the opposite sign) at a slightly faster rotation rate. The parameters of the anti-solar DR fits along with their errors, are summarised in Table 2.

4.2. Poleward meridional flow

Latitudinal spot changes can also be quantified from the time-series Doppler images. Meridional motion of surface features can be derived by cross-correlating the corresponding longitude stripes along the meridian circles. For this we use only the hemisphere of the visible pole because, in general, Doppler imaging is less reliable below the stellar equator once the inclination of the rotational axis is below approximately 60°. Again, we use only the consecutive but contiguous image pairs, i.e., #1−#3, #2−#4, #3−#5 and #4−#6. We take a correlation segment centred at 45° latitude with a predefined length from the initial image and, by shifting it from the equator to the pole on the other image, we calculate the cross-correlation function. Doing the same for each longitude we obtain the longitudinal distribution of these latitudinal ccfs, i.e., a latitudinal ccf map. We repeat this procedure for each Doppler image pair and the resulting latitudinal ccf maps are averaged. The correlation maxima for each longitudinal stripe are fitted with a Gaussian and the Gaussian peaks represent the best correlating latitudinal shifts.

The resulting latitudinal ccf maps in Fig. 2 indicate a joint poleward migration trend of $4.0 \pm 0.2°$ per rotation cycle (19.6 days) for the Ca images, $2.5 \pm 0.4°$ for the Fe images, and $4.1 \pm 0.3°$ for the average Ca+Fe images. It is tempting to interpret the poleward migration of surface features as a tracer of a global meridional flow on σ Gem with an average velocity for the Ca, Fe and Ca+Fe images of $346 \pm 12\,\mathrm{m\,s^{-1}}$, $216 \pm 28\,\mathrm{m\,s^{-1}}$, and $351 \pm 25\,\mathrm{m\,s^{-1}}$, respectively, and for a stellar radius of $R = 12.3\,R_\odot$. However, to conclusively establish such an interpretation, the pattern must be reproducable at other epochs.

5. Discussion and conclusions

Over recent years, a growing number of studies have reported differential rotation of solar-type equatorial acceleration on the (sub)giant components of RS CVn-type stars, e.g. for V711 Tau (Donati et al. 2003; Petit et al. 2004b), for IL Hya (Weber & Strassmeier 2005), and for ζ And (Kővári et al. 2007), as well as of anti-solar type deceleration of the equatorial zone for UZ Lib (Oláh et al. 2003), for IL Hya (Weber et al. 2003), and for HK Lac, HD 208472 and IM Peg (Weber et al. 2005). In all cases
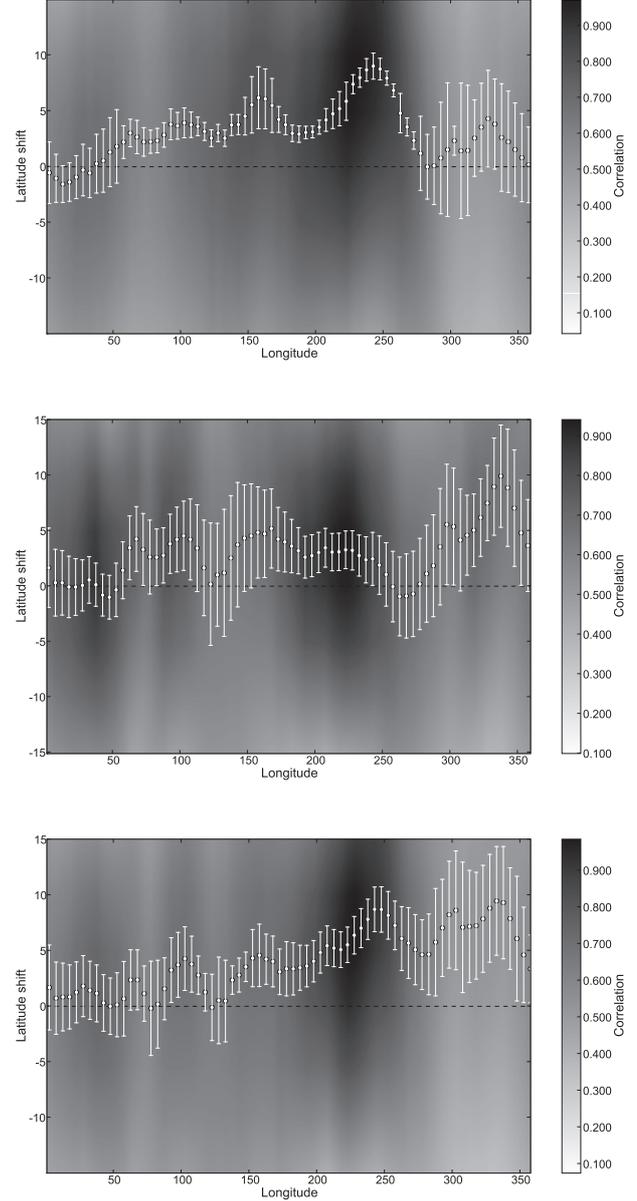
Fig. 2. Latitudinal ccf maps for the Ca images (*top panel*), for the Fe images (*middle panel*), and for the the combined Ca+Fe (*bottom panel*) Doppler images. The background grey scale quantifies the correlation strength. Best correlating latitudinal shifts are marked with dots (Gaussian peaks), the corresponding error bars reflect the fitted Gaussian FWHMs. The average positive shift suggests common poleward migration with an equivalent velocity of $2.5-4.1°$ per rotation cycle.

the derived DR parameters are relatively small compared to the solar value, regardless of the sign, and for some objects (IL Hya, V711 Tau) both solar and anti-solar patterns were derived at

different times. On the other hand, the strongest DR parameters of about 1.5 times the solar shear were derived for single giants: the FK Com-type HD 199178 (Petit et al. 2004c), and the effectively single KU Peg (Weber & Strassmeier 2001, note that a weaker α of 0.09 was also derived). A quite strong anti-solar differential rotation with $\alpha = -0.125$ was found by Strassmeier et al. (2003) for HD 31993, which is also a single giant. Although the sample above is poor for an established conclusion, yet, it suggests an important role of the tidal forces in controlling DR of the evolved components in RS CVn systems.

Standard hydrodynamical models in the past could not account for anti-solar type DR and the physical processes behind this phenomenon is still unclear. A revision of the theory was suggested recently by Kitchatinov & Rüdiger (2004), who included some additional drivers to maintain fast meridional flow, which would result in anti-solar type DR. Such driver candidates are large-scale thermal inhomogeneities and/or tidal effects in close binary systems. The spotted giant component of the RS CVn-type σ Gem fulfils both criteria. Kitchatinov & Rüdiger (2004) gave a rough estimation for the minimum value of the meridional flow component $u_{\min}^{m}$ which could already support anti-solar DR:

$$u_{\min}^{m} \approx 30 \frac{l^2}{\tau R}, \qquad (2)$$

where l is the mixing length and τ the corresponding turnover time-scale. Taking $l = 5.6 \times 10^8$ m and $\tau = 6.7 \times 10^5$ s (Paternò et al. 2002) with $R = 8.6 \times 10^9$ m (cf. Table 1) yields $u_{\text{crit}}^{m} = 1.6$ km s^{-1}, which is about five times more than what we measured in Sect 4.2 ($u_{\text{ccf}}^{m} \approx 300$ m s^{-1}, if the measurement is interpreted as a poleward migration velocity). On the other hand, taking a larger turnover time of $\tau = 5.5 \times 10^6$ s (cf. Gunn et al. 1998) with a correspondingly larger l of 7×10^8 m would yield $u_{\text{crit}}^{m} = 0.3$ km s^{-1} which is in the order of u_{ccf}^{m}, and thus, may support the analytical estimation of the sufficient angular momentum transport in Eq. (2).

We conclude that we have found anti-solar differential surface rotation on the active K giant σ Gem with a shear of -0.022 ± 0.006 and a lap time of ≈ 900 days. Evidence is presented for a poleward meridional migration of spots which, if interpreted due to an underlying meridional flow, would amount to ≈ 300 m s^{-1}.

References

Balthasar, H., Vazquez, M., & Woehl, H. 1986, A&A, 155, 87
Donati, J.-F., & Collier Cameron, A. 1997, MNRAS, 291, 1
Donati, J.-F., Collier Cameron, A., & Petit, P. 2003, MNRAS, 345, 1187
Gunn, A. G., Mitrou, C. K., & Doyle, J. G. 1998, MNRAS, 296, 150
Kitchatinov, L. L., & Rüdiger, G. 2004, AN, 325, 496
Kővári, Zs., Strassmeier, K. G., Bartus, J., et al. 2001, A&A, 373, 199
Kővári, Zs., Strassmeier, K. G., Granzer, T., et al. 2004, A&A, 417, 1047
Kővári, Zs., Weber, M., & Strassmeier, K. G. 2005, in Cool Stars, Stellar Systems and the Sun 13, 5−9 July 2004, Hamburg, Germany, ESA-SP-560, Vol. II, 731
Kővári, Zs., Bartus, J., Strassmeier, K. G., et al. 2007, A&A, 463, 1071
Maunder, E. W., & Maunder, A. S. D. 1905, MNRAS, 65, 813
Oláh, K., Jurcsik, J., & Strassmeier, K. G. 2003, A&A, 410, 685
Paternò, L., Belvedere, G., Kuzanyan, K. M., & Lanza, A. F. 2002, MNRAS, 336, 291
Petit, P., Donati, J.-F., & Collier Cameron, A. 2004, AN, 325, 221
Petit, P., Donati, J.-F., Wade, G. A., et al. 2004, MNRAS, 348, 1175
Petit, P., Donati, J.-F., Oliveira, J. M., et al. 2004, MNRAS, 351, 826
Shibahashi, H. 2007, AN, 328, 264
Švanda, M., Zhao, J., & Kosovichev, A. G. 2007, Sol. Phys., 241, 27
Strassmeier, K. G., Kratzwald, L., & Weber, M. 2003, A&A, 408, 1103
Strassmeier, K. G., Carroll, T. A., Rice, J. B., & Savanov, I. S. 2007, Mem. S. A. It., in press
Vida, K., Kővári, Zs., Švanda, M., et al. 2007, AN, submitted
Weber, M. 2004, Ph.D. Thesis, University of Potsdam
Weber, M., & Strassmeier, K. G. 2001, A&A, 373, 974
Weber, M., Strassmeier, K. G., & Washuettl, A. 2003, in The Future of Cool-Star Astrophysics, 12th Cambridge Workshop on Cool Stars, Stellar Systems, and the Sun (2001 July 30−August 3, Boulder, Colorado), ed. A. Brown, G. M. Harper, & T. R. Ayres (University of Colorado), 922
Weber, M., Strassmeier, K. G., & Washuettl, A. 2005, AN, 326, 287
Weber, M., & Strassmeier, K. G. 2005, in Cool Stars, Stellar Systems and the Sun 13, 5−9 July 2004, Hamburg, Germany, ESA-SP-560, Vol. II, 1029